Field-induced phase transition, weak ferromagnetism, and metamagnetic transition in the underdoped PrBCO cuprate

Mahieddine Lahoubi[1], Shengli Pu[2], Weinan Liu[2] and Zhe Yang[2]

[1] Badji Mokhtar Annaba University, Faculty of Sciences, Department of Physics, PO Box 12, 23000, Annaba, Algeria
[2] University of Shanghai for Science and Technology, College of Science, Shanghai 200093, China
Emails: mlahoubi@hotmail.fr & mlahoubi@gmail.com

Abstract. In the present paper we report on the magnetic properties of nonsuperconducting $PrBa_2Cu_3O_{6.44}$ ($PrBCO_{6.44}$) ceramic sample under high DC magnetic fields up to 11 and 16 T, respectively in the range of temperatures 1.35-20 and 2-12 K. By analyzing the *T*-dependence of magnetization and its derivatives, we reveal significant field-induced effects. Anomalies are observed at the low-critical point (T_{cr} = 4-5 K), spin reorientation phase transition temperature (T_2 = 6.5 K), and Néel temperature (T_N(Pr) = 9 K) of the Pr antiferromagnetic order. Arrott plot analysis identifies field-induced phase transitions at critical fields H_{cr1} ~ 3.3 T and H_{cr2} ~ 7.5 T. Among novel findings, we observe a weak ferromagnetic-like behavior that persists well above T_N(Pr). By employing a sensitive vibrating sample magnetometer 2 T, we detect weak field-induced metamagnetic phase transitions at threshold fields H_t below 0.16 T from 100.7 K down to 4 K and this, after crossing T_N(Pr). Our results shed light on the weak ferromagnetism coexisting with predominated antiferromagnetism in both Pr and Cu(2) subsystems, and provide insights into the complex Pr-Cu(2) interactions in this underdoped PrBCO cuprate.

1. Introduction

The magnetic properties of the praseodymium based compounds such the nonsuperconducting $PrBa_2Cu_3O_{6+x}$ ($PrBCO_{6+x}$ or PrBCO) materials remain an outstanding problem in the field of cuprates magnetism [1, 2]. Their studies can permit until now interesting perspectives into our understanding of "magnetic superconductors" such the REBCO bulks and films (where RE is a rare earth, Y or La) for a number of reasons. One of the first unusual features of the magnetism in PrBCO is the long-range antiferromagnetic (AFM) order in the Cu(2) sublattice as well as in the Pr sublattice. Superconductivity is not found for any *x* in samples of $PrBCO_{6+x}$ prepared by standard methods [3], and the AFM order in Cu(2) sublattice lies at a Néel temperature $T_N\{Cu(2)\}(x)$ ~ 300 K which depends only weakly on *x*, throughout the entire range of oxygen doping $0 \leq x \leq 1$ [1, 2]. This behavior contrasts strongly with that of $YBCO_{6+y}$ in which the value of $T_N\{Cu(2)\}(y)$ declines in value from 410 K at $y \sim 0.1$ to zero at $y \sim 0.4$, and for $y > 0.4$ a superconducting phase appears with a maximum superconducting transition temperature T_C of about 92 K at $y \sim 0.95$. For the magnetic transition which occurs additionally in the Pr sublattice, the Néel temperature T_N(Pr) takes unexpected values in the temperature range of 14-20 K and 7.5-12.5 K, respectively for the optimally (OP) ($0.50 < x < 1$) or over (OV) ($x = 1$) doped states in the orthorhombic phase, and for the underdoped (UN) ($0 < x < 0.50$) or oxygen-depleted (DE) ($x = 0$) states in the tetragonal phase [4 and refs. therein]. They magnetic properties are strikingly different from those of other members of the REBCO family with T_N(Pr) values appear an order of magnitude higher than for other RE ions with T_N(RE) = 0-2 K. The

AFM phase of the spins of the Cu(2) sublattice in PrBCO is the well-known 'AFI phase' [5], in which the spins on the Cu(2) sites within the CuO layers align antiparallel to their nearest neighbours along all three crystallographic axes, as it was identified in neutron diffraction experiments on two crystals on UN (x = 0.35) and OP (x = 0.92) states. The magnitude of the saturated ordered moment on the Cu(2) sublattice μ{Cu(2)} ~ 0.6 μ_B was found at 30 K, and no ordered moment was detected on the Cu(1) sublattice [5]. In the second magnetic phase, corresponding to the low-temperature phase below T_N(Pr) which is equal respectively at 11 and 19 K, noncollinear magnetic structures were found to occur in the Pr sublattice. Based on another AFM model labeled as 'AFMIII', it has been established the existence of an angle to the ***ab***-plane of about 38° and 55° for μ(Pr) ~ 1.15 and 0.6 μ_B, respectively for UN and OP samples [4]. They were interpreted theoretically in terms of Pr-Pr exchange, pseudodipolar interactions due to the Pr-Cu(2) magnetic coupling [5, 6], crystal field (CF), and quadrupolar interactions of the Pr-4f electrons [7, 8]. High-resolution neutron-scattering and resonant X-ray scattering made on OP and OV single crystals (x = 0.92, ~ 1) with T_N(Pr) = 17-20 K [4 and refs. therein] revealed that the change in the AFM structure of the Cu(2) sublattice is due to the spin reorientation phase transition (SRPT) at T_2 = 9-13 K. This SRPT is accompanied by a doubling of the magnetic unit cell along the ***c***-axis with a crossover from incommensurate to commensurate of the two sublattices at ~ 4.4 K, i.e., close to the low-critical point T_{cr} = 4-5 K where anomalies and a substantial weak ferromagnetic (WFM) behavior have been observed on UN [9] and OP [10] samples. However, there are in the literature review few studies on the magnetic properties which establish clearly the existence of the WFM behavior over a wide range of T, while previous studies have reported only the H-T magnetic phase diagram (MPD) below T_N(Pr) = 15.0 K of an OP single crystal [11].

Our study aims to elucidate the existence of field-induced phase transitions and to detect the emergence of WFM behavior that remains little explored experimentally for PrBCO in the UN state, unlike the case of a PrBCO in OP state [12]. To achieve this goal, we present a detailed study of the magnetic properties of this compound under high and very low magnetic fields.

2. Experiments

The data of isothermal magnetization, M versus H up to 11 T (maximum resolution of 10^{-4} emu) in the 1.35-20 K range, and up to 16 T (maximum resolution of 10^{-3} emu) in the 2-12 K range were obtained on a $PrBCO_{6+x}$ ceramic sample prepared by standard solid-state reaction method. The structure and the grain size of the sample which is a parallelepiped (L = 2.806 mm × h = 1.816 mm × l = 2.30 mm), are characterized by XRD and scanning electron microscopy, and the sample is found to be single phase and belongs at the tetragonal space group (*P/4mmm*). A thermogravimetric analysis has been done to check the oxygen content x which was found equal to 0.44.The field H was produced by the two magnetometers based on superconducting coils already described in [9, 10, 12]. The susceptibility, dM/dH versus H was deduced by simple numerical differentiation, and the derivative, dM/dT versus T was collected using the 11 T magnet. Few M data, obtained using a VSM2T which has a good maximum resolution of 10^{-7} emu and stability of regulation of the order of 0.01 K [9], are reported.

3. Results and discussion

The M-H curves for H up to 11 and 16 T are displayed in figures 1, 2, respectively. Above a slightly curved part for H < 1 T and for all values of T, we see a sublinear behavior with the appearance of a small hysteresis effect in the M shape variation between increasing and decreasing H. We notice that M versus H at 2 K never reaches saturation neither at 10 T, nor even at 14.6 T, the maximum achievable value of H using the 16 T magnet. The unsaturated behavior of M-H curves at 1.35 and 2 K, leads us to consider an AFM/WFM type nature of the magnetic properties of our sample. The largest value that M takes at H = 14.0 T is only 38.8% of the Pr^{3+} saturation moment, which can be compared to 31.3% obtained under identical experimental conditions on the sample with x = 0.95 [12]. Previous M at 5 K for both H // ***c***-axis and H // ***ab***-plane [11] have lead at 4.5 T (H was limited to 4.8 T), M_c = 15.72 and M_{ab} = 10.23%, respectively. A comparison with our M data at 4 and 5 K gives for H = 4.5 T the average value of 15.71% and suggests that the sample is aligned along the ***c***-axis.

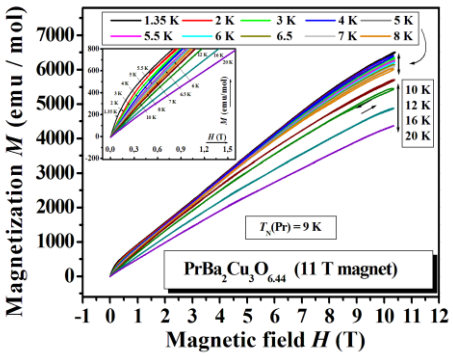

Figure 1. M vs H up to 11 and 1.5 T (for the zoomed view in the inset) at T = 1.35-20 K.

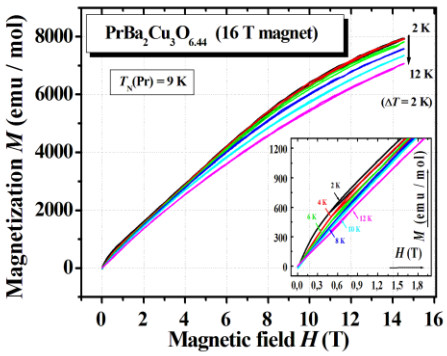

Figure 2. M vs H up to 16 and 1.5 T (for the zoomed view in the inset) at T = 2-12 K.

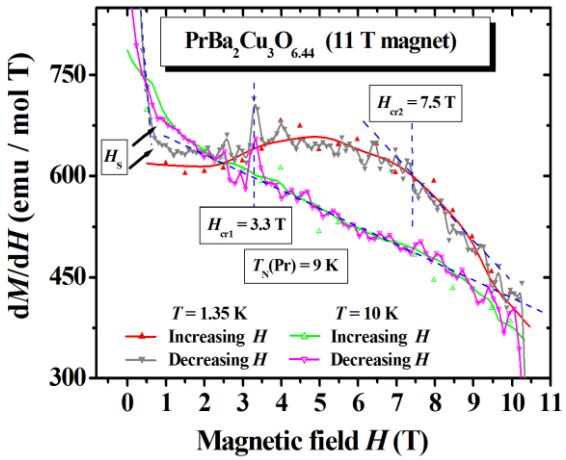

Figure 3. Susceptibility dM/dH vs H up to 11 T at 1.35 and 10 K. Critical fields H_{cr1}, and H_{cr2} associated to FIPTs appear at 1.35 K in decreasing H. Only H_{cr1} is observed at 10 K.

Typical curves of susceptibility dM/dH versus H up to 11 T at 1.35 and 10 K are shown in figure 3.

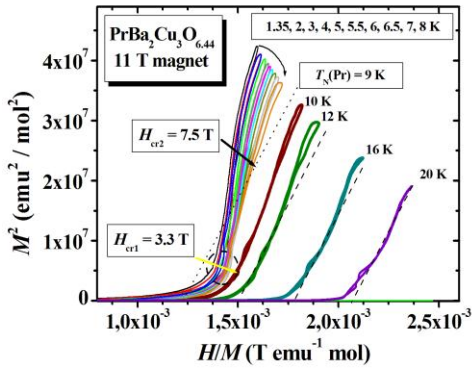

Figure 4. M^2 vs H/M with H up to 11 T below and above T_N(Pr) (T = 1.35-20 K).

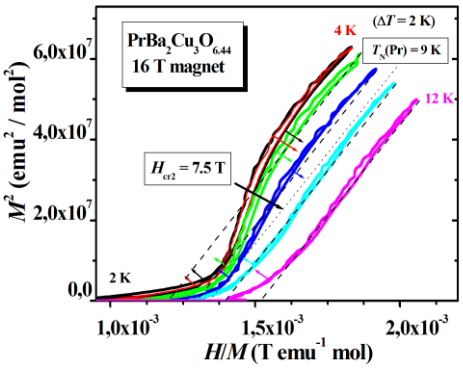

Figure 5. M^2 vs H/M with H up to 16 T below and above T_N(Pr) (T = 2-12 K).

We know that the attainable maximum value of the field H is about 10 T in the case of the 11 T magnet. This is due to the importance of the amplitude of the field fluctuation in the range of 10-11 T. At 1.35 K, field-induced phase transitions (FIPTs) are detected at two critical fields: at H_{cr1} ~ 3.3 T, only in decreasing H with a sharp peak as a feature of a first-order transition which remains at 10 K; at H_{cr2} ~ 7.5 T, a value estimated from the inflection point due to the change of slope at 1.35 K which seems to disappear at 10 K both in increasing and decreasing H. Generally, Arrott plots have been widely used for determining Curie temperatures in magnetic materials. Arrott plot method is an alternative means of analysis, which appears more useful to investigate critical fields in the neighbourhood of FIPTs. The curves of the square of the isothermal magnetization M^2 calculated as a function of H/M and for fixed T are displayed in figures 4, 5, respectively for H up to 11 and 16 T. A modest hysteresis, which occurs at 1.35 and 2 K, seems to decrease with increasing T. The following features are of interest: (i) the curves above the oblique and dotted line at 9 K, i.e., close to T_N(Pr), are parallel straight lines up to the higher fields, and whose abscissa at the origin is equal to $1/\chi$; (ii) below 9 K, the curves show a 'S-shape behavior'. They intercept a slope identical to that observed for $T \geq 9$ K, just at an inflection point which occurs at H_{cr2} = 7.5 T at 1.35 and 2 K, and reinforce the result that T_N(Pr) ~ 9 K. The variation of H_{cr2} with T is indicated by the solid black arrow in both figures 4, 5. The curves M^2 versus H/M with H up to 11 T shown in figure 4 are able to access to the zoomed view of the region around H_{cr1} = 3.3 T, and this, due to a better resolution compared to that of the 16 T magnet. The noticeable kink at H_{cr1} identified inside the dashed circle can be followed by the yellow arrow which starts at 1.35 K. Below T_N(Pr), the 'S-shape behavior' of the curves remains and the increase of the shape of the convex curvature as T decreases down to 1.35 and 2 K, is accompanied from H_{cr2} by the development of a concave curvature in the higher field part.

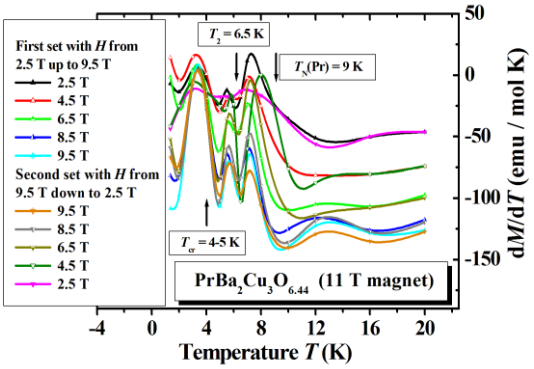

Figure 6. dM/dT vs T in the 1.35-20 K range for two sets of H in the 2.5-9.5 T range, using the 11 T magnet. Significant magnetic-field effects occur around T_{cr}, T_2, and T_N(Pr).

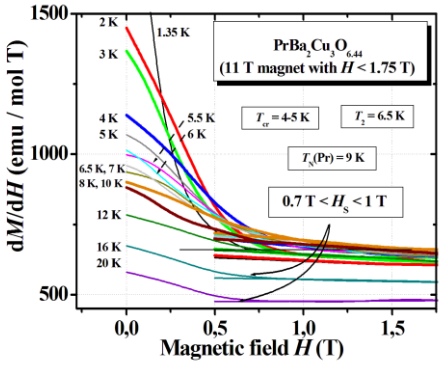

Figure 7. dM/dH vs H up to 1.75 T using the 11 T magnet. For H in the range of 0.7 T < H_S < 1 T, an increase is observed for T < 20 K with a high-speed variation for $T < T_{cr}$.

All these Arrot plots confirm the existence of the critical fields H_{cr1} and H_{cr2} for which their associated transition lines exhibit an almost temperature-independent variation up to the T_2-point, and seem to vanish abruptly near T_N(Pr). The curves of dM/dT versus T are shown in figure 6 for two sets of H which takes the five values of 2.5, 4.5, 6.5, 8.5, and 9.5 T, firstly from 2.5 up to 9.5 T and secondly from 9.5 down to 2.5 T. There is no visible difference between the two sets of curves between 1.35 K and 20 K. The shape of the wavelike curve around T_N(Pr) is strongly depressed in size for H from 2.5 up to 9.5 T towards a pronounced convex anomaly upwards. The small wavelike curve around T_2 shows an increase of its profile for $H \geq 6.5$ T. The rounded peak at T_{cr}, appears fairly affected as H reaches 9.5 T. The presence of H_{cr1} ~ 3.3 T is perceptible again on the first set when H increases from 2.5 up to 4.5 T. We can conclude that we found for the first time on an UN sample two transition lines associated to the critical fields H_{cr1} and H_{cr2} which are in good agreement respectively with those reported in the previous H-T MPD constructed by Narozhnyi *et al*. [11] for both H // ***ab***-

plane and H // ***c***-axis of an OP single crystal sample, and with our recent findings on an OP ceramic sample [12]. We mention that we have detected the small and almost vertical transition lines which emerge from the T_2 and T_{cr}-points, in agreement with those previously observed in the derivative of the paraprocess susceptibility χ_H, dχ_H/dT for H = 2, 4, and 6 T [9].

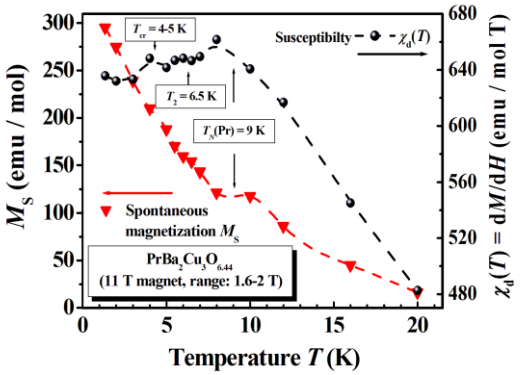

Figure 8. Curves of the spontaneous magnetization, M_S and differential susceptibility, χ_d vs T up to 20 K deduced with the M data obtained using the 11 T magnet. Anomalies are observed around T_{cr}, T_2, and T_N(Pr).

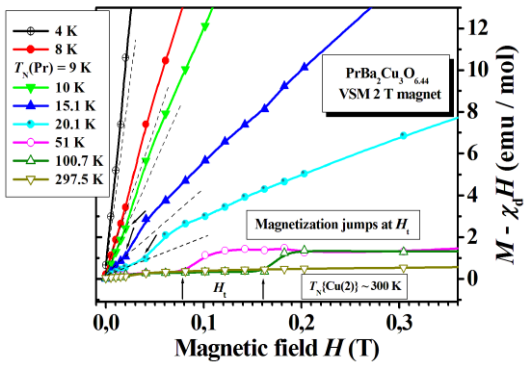

Figure 9. Curves of $M - \chi_d H$ vs H up to 0.36 T. Using the VSM2T magnet, magnetization jumps due to FIMPTs occur at threshold fields $H_t \leq 0.16$ T for $T \leq 100.7$ K (< T_N{Cu(2)} ~ 300 K [4]) down to 4 K after crossing the Néel point T_N(Pr).

The dM/dH curves are plotted now for various temperatures between 1.35 K and 20 K in figure 7, which is in essence complement to figure 3, as function of a low-field H up to 1.75 T (i.e., $H < H_{cr1}$) using the 11 T magnet. Above T_N(Pr), the curves show a slight increase for H in the range of 0.7 T < H_S < 1 T, where H_S is the specific field above which a WFM-like contribution settles into both AFM regimes. As T decreases, dM/dH increases significantly. Below T_{cr}, dM/dH exhibits a high-speed increase down to 1.35 K. The high accuracy of the dM/dH curves is related to the linear-field dependence in the small H_S-H_{cr1} field-range of the associated M-H curves. Then, they may be represented in the entire T-range by the equation $M_S + \chi_d H$. The spontaneous magnetization, M_S and differential susceptibility, χ_d are obtained by extrapolation to zero-field from the linear parts of the M-H curves in the $H_S < H \leq 2$ T field-range. Their values are respectively equal to 295.2 emu mol^{-1} and 635.8 emu mol^{-1} T^{-1} at 1.35 K, and 16.1 emu mol^{-1} and 482.6 emu mol^{-1} T^{-1} at 20 K.

The T-dependences of M_S and χ_d are plotted in figure 8 for PrBCO$_{6.44}$. They decrease with increasing T from 1.35 up to 20 K presenting particular features on crossing T_N(Pr). It can be seen that M_S does not vary with T like that of ferromagnetic (FM) materials but decreases as the inverse of T, like a paramagnetic (PM) system with a shape change when crossing T_N(Pr). On the contrary, χ_d has a behavior practically analogous to that of AFM materials. Its behavior may seem somewhat contradictory. In the PM region, we define χ by the ratio M/H, and when a permanent magnetic moment appears, χ must tend towards infinity, or at least become very large, as in the case of FM materials. However, the χ_d curve shows a nearly "horizontal" portion with visible anomalies at T_{cr} = 4-5 K, and T_2 = 6.5 K, with a shape change when crossing T_N(Pr), and exhibits above T_N(Pr), a fast decay quasi similar to that observed in PrBCO$_{6.95}$ in the same range of T used in [12]. Previous investigations based on X-ray magnetic circular dichroism provided evidence of a field-induced out-of-CuO$_2$ plane Cu(2) spin moments in an OP YBCO$_{6+y}$ film with T_C = 90 K [13]. At 9 K and 4 T, the Cu(2) spins are canted out-of the CuO$_2$ planes. As T increases, the ***c***-axis spin moment, i.e., perpendicular to the CuO$_2$ superconducting layers, decreases with T exhibiting an exponential decay. We observe that M_S presents an inverse variation with T and survives well above T_N(Pr) with a finite quantity for χ_d. This is due partially to the out-plane Cu(2) spins which appear not coupled with the AFM order of the Cu(2) spins which have the same AFM structure found in an UN YBCO$_{6+y}$. These

results suggest that the Pr^{3+} moments appear not coupled to the Pr AFM ordering but coupled to the out-plane Cu(2) moments, and this, despite the intrinsic both canted orders observed below T_N(Pr) [5]. We can argue that such *T*-dependence resembles with that reported in the case of the OP sample [12]. This interpretation of the results, where a WFM-like behavior appears and persists well above T_N(Pr), is in agreement with the previous model based on the significant role of the Pr-Cu(2) coupling used to describe the magnetic, electronic, and optical properties in PrBCO in UN and DE states [5, 6, 8, 14, 15]. Finally, we plotted in figure 9 the curves $M - \chi_d H$ versus H obtained in fields lower than 0.36 T, using the VSM2T magnet in the 4-297.5 K range. They show magnetization jumps associated to weak field-induced metamagnetic phase transitions (FIMPTs) at threshold fields $H_t \leq 0.16$ T, (i.e., well below H_S) for $T \leq 100.7$ K (< T_N{Cu(2)} ~ 300 K) [4] down to 4 K after crossing the Néel point T_N(Pr), with the consequence of the appearance of a possible remanent magnetization M_r, and initial susceptibility, χ_r.

4. Conclusion

All these features have led us to conclude that the complex magnetic properties for the $PrBCO_{6.44}$ cuprate is related to the significant role of the Pr-Cu(2) coupling below T_N(Pr) = 9 K down to 1.35 K which seems to continue well beyond T above T_N(Pr) = 9 K, and this, up to 20 K, the most higher value of T used in our high-field magnetization study. Our results provide compelling evidence for the existence of the WFM behavior, FIPTs and weak FIMPTs in this underdoped PrBCO compound and future studies may explore the impact of these findings. Further experimental extensions with magnetic fields large enough (H_{max} >> 16 T) and under FC or zero field cooling conditions applied on single crystals are required to observe the saturation regime and to map out the *H-T* MPD. By using the VSM2T, it will be also useful to follow in the whole range of T up to room temperature the variations of M_r, χ_r, and H_t.

5. References

[1] Akhavan M 2002 *Physica* B **321** 265
[2] Lynn W, Rosov N, Barilo S N, Kurnevitch L and Zhokhov A 2000 *Chin. J. Phys.* **38** 286
[3] Blackstead H A and Dow J D 2000 *Solid State Commun.* **115** 137
[4] Boothroyd A T 2000 *J. Alloys Compd.* **303–304** 489
[5] Boothroyd A T *et al.* 1997 *Phys. Rev. Lett.* **78** 130
[6] Maleev S V 1998 *JETP Lett.* **67** 947
[7] Hilscher G *et al.* 1994 *Phys. Rev. B* **49** 535
[8] Kiss A and Simon F 2010 *Phys. Rev. B* **82** 174413
[9] Lahoubi M 2018 *Physica B* **536** 12
[10] Lahoubi M 2018 *IEEE Trans. Appl. Supercond*. 28 7200405
[11] Narozhnyi V N *et al*. 1999 *Physica C, Supercond.* **312** 233
[12] Lahoubi M, Pu S, Liu W and Yang Z 2024 *IEEE Magn. Lett.* **15** 2500105
[13] De Luca G M *et al*. 2010 *Phys. Rev. B* **82** 214504
[14] Lister S J S *et al.* 2001 *Phys. Rev. Lett*. **86** 5994
[15] Zibold A *et al*. 1997 *Phys. Rev. B* **55** 11096

Acknowledgments

This work was supported in part by the Algerian Ministry of Higher Education and Scientific Research through the last CNEPRU project approved for the L.P.S. Laboratory under Grant D01120120111, and in part by an earlier cooperation between Badji Mokhtar Annaba University, Algeria and University of Joseph Fourier-CNRS-Grenoble, France (CMEP 95MDU343), where Prof. M Lahoubi obtained several measurement periods for the use of the magnetic-field installations. Prof. S Pu is acknowledged for his collaboration without any funding or grants in the basis of joint activities whose major topics are “magnetism in Pr compounds with garnet and cuprate structures and magnetooptical and magnetophotonic devices based on magnetic iron (and non iron) garnets and magnetic fluids”.